BioOne COMPLETE

Ice Propagation in Dehardened Alpine Plant Species Studied by Infrared Differential Thermal Analysis (IDTA)

Authors: Hacker, Jürgen, and Neuner, Gilbert

BioOne Complete (complete.BioOne.org) is a full-text database of 200 subscribed and open-access titles in the biological, ecological, and environmental sciences published by nonprofit societies, associations, museums, institutions, and presses.

BioOne sees sustainable scholarly publishing as an inherently collaborative enterprise connecting authors, nonprofit publishers, academic institutions, research libraries, and research funders in the common goal of maximizing access to critical research.

Ice Propagation in Dehardened Alpine Plant Species Studied by Infrared Differential Thermal Analysis (IDTA)

Jürgen Hacker*† and
Gilbert Neuner*‡

*Institute of Botany, University of Innsbruck, Sternwartestraße 15, 6020 Innsbruck, Austria
†Corresponding author: juergen.hacker@uibk.ac.at
‡gilbert.neuner@uibk.ac.at

Abstract

Infrared differential thermal analysis (IDTA) was used to study ice propagation and whole plant freezing patterns in dehardened intact individuals of various alpine plant species, including a shrub (*Rhododendron ferrugineum*), a herbaceous plant (*Senecio incanus*), a cushion plant (*Silene acaulis*), and two graminoids (*Poa alpina* and *Juncus trifidus*). Freezing patterns differed markedly among species and reflected peculiarities of the shoot structure and the vascular system. In graminoids, each single leaf required a separate ice nucleation event, as the polystele prevents ice propagation between leaves via the stem. Additionally, enhanced supercooling resulted in a temperature range of whole plant freezing of up to 10°C, which corroborates the high summer frost resistance of graminoids. This could have ecological significance for frost survival. In contrast, in dicotyledonous species one nucleation event was usually sufficient for whole plant freezing. Controlled ice-seeding experiments on leaves with droplets of water and bacterial water suspension (*Pseudomonas syringae*) showed that ice propagation into the leaf tissue from the surface was inhibited as long as the leaves were undamaged. The rate of ice propagation in veins was significantly higher at lower temperatures and reached up to 24 cm s^{-1} in *J. trifidus*, which is much higher than reported in earlier findings. Ice propagation in graminoids was much faster, which may indicate that ice propagates within the protoxylem lacunae of large vessels.

Introduction

Freezing stress is the first environmental filter a species has to pass through to become alpine (Körner, 1999). In European temperate alpine regions, sufficient frost hardening and snow cover (Sakai and Larcher, 1987) usually ensure frost survival in winter with predictable frost events. The situation is different throughout the growing period in summer when a low frost resistance coincides with unpredictable freezing events (Taschler and Neuner, 2004). After bud burst, during leaf expansion, alpine plant species are most frost susceptible and may even be damaged by frost at their natural growing sites (Taschler and Neuner, 2004). Small plants dominate the alpine habitat; the smallness causes a decoupling of plant body temperature from ambient (Körner, 1999). During the day, this usually produces a warmer microclimate, advantageous in a usually cold alpine environment. During the night, radiative heat loss from alpine plants is significant (Jordan and Smith, 1994) with leaves cooling by up to 8°C below ambient air temperature. Under calm conditions with low convection, small plants can be exposed to significantly lower temperatures than tall species due to long wave thermal energy dissipation. This increases the likelihood of frost damage and hence increases the need for specific frost survival mechanisms. Ice propagation throughout the plant can be considered ecologically significant for frost survival, particularly for the alpine species that may be exposed to freezing temperatures during their active growing period.

In earlier studies ice propagation in woody plants (Wisniewski et al., 1997; Workmaster et al., 1999; Carter et al., 2001; Ball et al., 2002; Sekozawa et al., 2004) and graminoids (Pearce and Fuller, 2001; Stier et al., 2003; Wisniewski et al., 2002a) was mainly studied by infrared video thermography (IRVT). IRVT investigations on ice propagation are rather rare for herbaceous plants (Wisniewski et al., 1997, 2002a), and are lacking totally for alpine plants. The recently developed technique of infrared differential thermal analysis (IDTA) of infrared images captured by a digital infrared camera has shown to be an efficient method for investigating freezing at the plant tissue level in leaves (Hacker and Neuner, 2007). In earlier investigations, ice propagation was mostly studied in detached plant parts, but rarely in whole plants. The smallness of alpine plants is hence advantageous as it allows an investigation of the freezing process in plants at the whole organism level. We investigated intact individuals from the predominating growth forms found in alpine habitats (woody shrub: *Rhododendron ferrugineum*; graminoids: *Juncus trifidus* and *Poa alpina*; herbaceous dicotyledonous species: *Senecio incanus* and *Silene acaulis* [cushion]) to determine ice propagation patterns at the whole organism level, employing the recently developed technique of IDTA (Hacker and Neuner, 2007). In the woody species investigated by Hacker and Neuner (2007), ice spread into the leaves after ice nucleation in the stem. Ice propagation was always associated with the leaf venation. This led to the suggestion that ice propagation initially occurs in the vascular tissue within vessels and tracheids. This implies a crucial role of the structure of the vascular system for ice propagation within the plant.

Freezing of plants can be initiated either by intrinsic or extrinsic ice nucleation (Wisniewski et al., 1997). Important extrinsic ice nucleators are ice nucleating active (INA) bacteria,

which induce ice formation at the surface of plants at high temperatures (Maki et al., 1974). Leaves are a large microbial habitat and are colonized by a variety of species with bacteria by far the most numerous (Lindow and Brandl, 2003). The existence of INA bacteria is not sufficient for extrinsic ice nucleation, as nucleators are only active in aqueous solutions and thus surface moisture is a prerequisite for extrinsic ice nucleation (Wisniewski et al., 2002a). In nature, plants are usually exposed to radiative cooling and are thus colder than the surrounding air. This causes the formation of dew on the cold plant surfaces when air is cooled below the dew point. External ice does not necessarily induce freezing inside the plant, as the external ice has to come into contact with internal spaces of the plant. Ice may propagate through stomates, damaged cuticle or other lesions into the plant (Wisniewski et al., 2002a). If there is no direct contact of extrinsic ice with surface water in the apoplast, ice propagation into the plant is inhibited and can hence cause no harm to the plant. As the experiments were conducted under convective cooling conditions, the influence of extrinsic ice nucleators present under radiative cooling conditions was additionally investigated. Droplets of water and bacterial suspension of INA bacteria were applied on intact and manually damaged leaf surfaces to simulate extrinsic ice nucleation.

Material and Methods

PLANT MATERIAL

Ice propagation was studied in various alpine plant species: an herb (*Senecio incanus* L.), a woody shrub (*Rhododendron ferrugineum* L.), two graminoids (*Poa alpina* L. and *Juncus trifidus* L.), and a cushion plant (*Silene acaulis* [L.] Jacq.). Plants of the investigated species were collected at natural sites in the central alps (around Mount Patscherkofel, 2240 m a.s.l., 47°12′32″N, 11°27′38″E) and potted in plastic containers (8 × 8 × 8.5 cm) filled with an alpine soil mixture. The potted plants were cultivated under natural environmental conditions in the Botanical Garden of the University of Innsbruck (600 m a.s.l., 47°16′4″N, 11°22′46″E). All experiments were conducted during summer, when the species were not frost hardened and exhibited their lowest frost resistance.

FREEZING TREATMENT

Potted plant samples were frozen in a convective freezing chamber with controlled temperature lowering at moderate rate of 4 K h^{-1}. Two additional measurements were done under radiative conditions for *R. ferrugineum* and *S. incanus*. Investigations were restricted to the aboveground parts of the plants. As the soil is a tremendous reservoir of heat, soil temperature lagged behind the temperature of aboveground plant parts and did not influence the freezing process. Thermocouples connected to a datalogger (CR10X, Campbell Scientific, Logan, Utah, U.S.A.) were placed at the surface of the analyzed organs to measure absolute temperatures. Plant samples were measured mainly with a dry surface to identify action sites of intrinsic ice nucleators. For testing the influence of extrinsic ice nucleation on whole plant freezing, leaf surfaces of *J. trifidus*, *P. alpina*, *R. ferrugineum*, and *S. incanus* were wetted either with tap water or with a suspension of INA bacteria in water for controlled ice nucleation at −2.5°C. The water and INA suspension were applied as 50 µL droplets either on intact or damaged leaf surfaces. The latter was produced manually with a razor blade, generating a grid of deep cuts enabling the contact of the external ice with internal tissues. The experiments included four surface treatments, and the number of individuals tested are as

follows (dry/water or INA suspension on an intact leaf surface/ water on a damaged leaf surface/bacterial suspension on a damaged surface): *J. trifidus* (6/1/0/1), *P. alpina* (11/3/2/3), *R. ferrugineum* (14/2/2/1), *S. incanus* (8/2/1/1), and *S. acaulis* (3/0/0/0).

A strain of INA bacteria with high ice nucleating activity (*Pseudomonas syringae*, strain 5176, DSMZ Deutsche Sammlung von Mikroorganismen und Zellkulturen GmbH, Braunschweig, Germany) was used for the bacterial suspension. The bacteria were cultivated monthly on nutrient agar (Nutrient Agar No 2, Fluka, Sigma-Aldrich Chemie GmbH, Buchs, Switzerland) in petri dishes at 22°C for 24 h and then stored at 5°C. The INA bacteria were applied as a bacterial suspension in distilled water containing several millions of bacterial cells (a count with the standard plate count method resulted in 144,000 bacterial cells µL^{-1} suspension).

INFRARED THERMOGRAPHY

Ice propagation in plants was measured with a digital infrared camera (FLIR Systems ThermaCAM^{TM} S60, FLIR Systems AB, Danderyd, Sweden) that was equipped with a close-up lens (LW 64/150) to achieve a high spatial resolution of 200 µm. The system was connected via a FireWire interface with a control computer for data transfer. Control of the infrared camera and data analysis was conducted with the software package ThermaCAM^{TM} Researcher (FLIR Systems AB, Danderyd, Sweden). The original infrared data were further analyzed by performing an infrared differential thermal analysis (IDTA) as described in Hacker and Neuner (2007). IDTA works in a fashion analogous to differential thermal analysis (DTA), where the sample temperature is compared with a reference temperature during the freezing treatment to detect the smallest temperature changes (Burke et al., 1976). IDTA is based on the subtraction of a reference image, captured just before the occurrence of freezing, from a sequence of images. The resulting differential images show only changes of temperature due to the release of heat during freezing; background temperature fluctuations are canceled out and smallest temperature changes can be visualized. In the resulting IDTA images, freezing is indicated by brightening of the tissue, while unfrozen areas remain black.

MEASUREMENT OF THE RATE OF ICE PROPAGATION

The rate of ice propagation in the veins of leaves was calculated by analysis of time series of IDTA images. The distance ice had propagated in the time span between IDTA images was measured by an image analyzing software (Optimas 6.5, Media Cybernetics, Bethesda, Maryland, U.S.A.). The rate of ice propagation was calculated as the ratio between distance and time.

STATISTICAL DATA ANALYSIS

Differences between means, tested by analysis of variance followed by the Bonferroni multiple comparisons post-hoc test (*P* < 0.01) and correlation analysis were performed by the statistical software SPSS (SPSS, Chicago, Illinois, U.S.A.). Means and standard errors were calculated for every species based on the number of replicates mentioned in the above section.

Results

SENECIO INCANUS

The sequence of IDTA images in a shoot of the herbaceous plant *S. incanus* (Fig. 1A) shows initial ice nucleation at −4.3 °C in

J. HACKER AND G. NEUNER / 661

the mesophyll of a leaf (Fig. 1B). Ice immediately spreads into the vascular bundles of this leaf and therein down the stem (Figs. 1C–1F). From the stem ice is propagated to all other leaves of the plant within 5.2 s (Figs. 1G–1J). During vascular ice propagation a second ice nucleation event was detected in the mesophyll of a second leaf (Fig. 1G). The reticulate venation pattern is only visible close to the moving ice front, but soon afterwards, it is blurred due to mesophyll freezing which starts immediately after ice has spread throughout the vessels. The veins end freely in the areole (Esau, 1965) as indicated by illumination of the outermost tips of the lobes of a leaf blade when ice has reached it (Figs. 1C–1G). At the beginning of mesophyll freezing, a brindled freezing pattern can be observed, indicating a faster water efflux in some regions of the leaf blade compared to others (Fig. 1H). This pattern is diminished within 30 s due to the release of heat in the whole leaf lamina (Fig. 1L). Intrinsic ice nucleation (dry leaf surface) occurred either in the leaf lamina (6 out of 8 individuals) or in the leaf petiole (2 out of 8 individuals), but never in the stem. Ice nucleation occurred in seven individuals in the mesophyll tissue and only once in the vascular tissue. This resulted in a time lag between ice nucleation and further ice propagation in the vascular tissue towards the leaf margin and the stem. Vascular freezing started mainly within 24.4 s after ice nucleation, but lasted up to 294 s in one individual. Freezing of the whole plant, i.e. further spread of ice from the stem to the unfrozen leaves, was finished in five individuals within 1 min, but could be delayed up to 35 min. Both the time lag between ice nucleation and vascular ice propagation and the time of whole shoot freezing was highly correlated with the freezing temperature. At higher ice nucleation temperatures (especially above −4°C), both processes were significantly delayed.

Freezing of droplets of water or INA suspension on an intact leaf lamina had no effect on the freezing process of the plant, as the ice was restricted to the frozen droplet at the surface and could not propagate into the plant. When the leaf lamina was damaged, ice of a frozen droplet of water or bacterial suspension could easily propagate into the plant and cause whole shoot freezing. The freezing pattern consisting of vascular and mesophyll freezing was not affected by the extrinsic source of ice nucleation.

The investigation of the freezing process of one individual of *S. incanus* under radiative cooling conditions *in situ*, showed the same freezing patterns as observed under convective cooling conditions (Fig. 2). During the ongoing experiment, snowfall set in, but had no effect on ice nucleation and the freezing pattern. Intrinsic ice nucleation occurred in a leaf lamina at −3.5°C and caused the freezing of two leaves (Figs. 2D–2K). The other leaves of the shoot remained unfrozen down to a leaf temperature of −4.5°C at the end of the experiment, when the plant was fully snow-covered.

Rhododendron ferrugineum

In the woody species *R. ferrugineum*, ice propagated throughout the entire shoot within 2 s, after ice nucleation had occurred in last year's stem at −7.3°C (Fig. 3). During ice propagation in the vascular tissue, the leaf venation pattern became visualized down to second-order side veins (Figs. 3B–3F). While in this year's leaves (the arrow in Fig. 3A marks the border between this and last year's leaves) the freezing pattern was clearly visible, in the last year's leaves IDTA images could not resolve the freezing process with the same resolution. Fully developed leaves are much thicker and the vascular bundles are embedded in a more compact tissue, hence heat, emitted during freezing of vascular bundles, is dispersed during the transmission to the leaf surface. In this year's leaves, the IDTA images did not differ, whether the lower or upper leaf side was exposed to the infrared camera. Immediately after vascular freezing the onset of mesophyll freezing blurred the venation pattern and showed a brindled freezing pattern at the beginning (Figs. 3G, 3H) and within one minute these differences were diminished (Fig. 3I).

The freezing pattern in *R. ferrugineum* was identical, when freezing was induced by extrinsic ice nucleation (Figs. 3J–3R). Ice nucleation occurred at −5.3°C in a water droplet, which was placed on a leaf with a damaged surface (Fig. 3J). Only 400 ms after freezing of the water droplet, vascular freezing of the leaf could be detected (Fig. 3L, indicated by an arrow). Subsequently ice spread into the stem and from there throughout the whole shoot (Figs. 3M–3R). A water droplet located on another leaf with damaged surface started to freeze as soon ice had spread into that leaf (Fig. 3Q). Frozen droplets of water or bacterial suspension on an intact leaf surface did not act as extrinsic nucleators and had no influence on the freezing process of the plant. This was also observed for the other investigated species with this surface treatment.

Poa alpina

IDTA images determined during ice propagation in leaves of the grass *P. alpina* show the parallel venation pattern typical of monocotyledonous plants (Fig. 4). Intrinsic ice nucleation occurred typically in the vascular tissue either at the boundary between the leaf sheath and the leaf blade (Fig. 4A, ice nucleation temperature −5.9°C) or at the base of the leaf blade (Fig. 4E, ice nucleation temperature −10.4°C). From there, ice propagated throughout the vascular system towards the leaf tip and the sheath base, and vascular freezing was followed by mesophyll freezing resulting in a brindled freezing pattern (Fig. 4D). Ice propagation was sometimes delayed for several seconds at the boundary between the leaf blade and leaf sheath, independently of which direction the ice front was moving in. The boundary between the leaf blade and leaf sheath is not present in early stages of leaf development, but is established when the ligule develops (Esau, 1965).

The vascular system of grass leaves consists of longitudinal bundles which are laterally interconnected by small bundles in a ladder-like manner (Esau, 1965); in *P. alpina* these lateral connections consist of single tracheids (Figs. 4K, 4L). This specific vascular system results in a combination of longitudinal and lateral vascular ice propagation (Figs. 4E–4J). As the distance between the parallel bundles is too small (92 ± 10 μm) to be spatially resolved by the infrared camera, lateral ice propagation cannot be visualized in IDTA images. However, occurrence of lateral ice propagation can be detected in continued ice propagation in a neighboring bundle (Fig. 4I and detail in Fig. 4J). The measured rate of lateral ice propagation is 20 times slower than the longitudinal rate, because it consists of a longitudinal and a lateral component.

Ice propagation was always restricted to a single leaf. Ice did not propagate further to other leaves via the stem. All leaves attached to a stem froze independently of each other requiring an autonomous ice nucleation event in each leaf. The influence of extrinsic nucleators was tested by applying water droplets and water droplets containing INA bacteria to intact and artificially damaged (razor blade incisions) leaves of *P. alpina*. Ice nucleation in water droplets occurred at −6.2 ± 0.2°C and in water droplets containing INA bacteria at the much higher temperature of −2.8 ± 0.2°C. After extrinsic ice nucleation in droplets applied to an intact leaf surface, ice always remained restricted to the plant surface. Similarly, ice propagation from frozen plant tissue to a droplet placed on the intact leaf surface was not detected. When
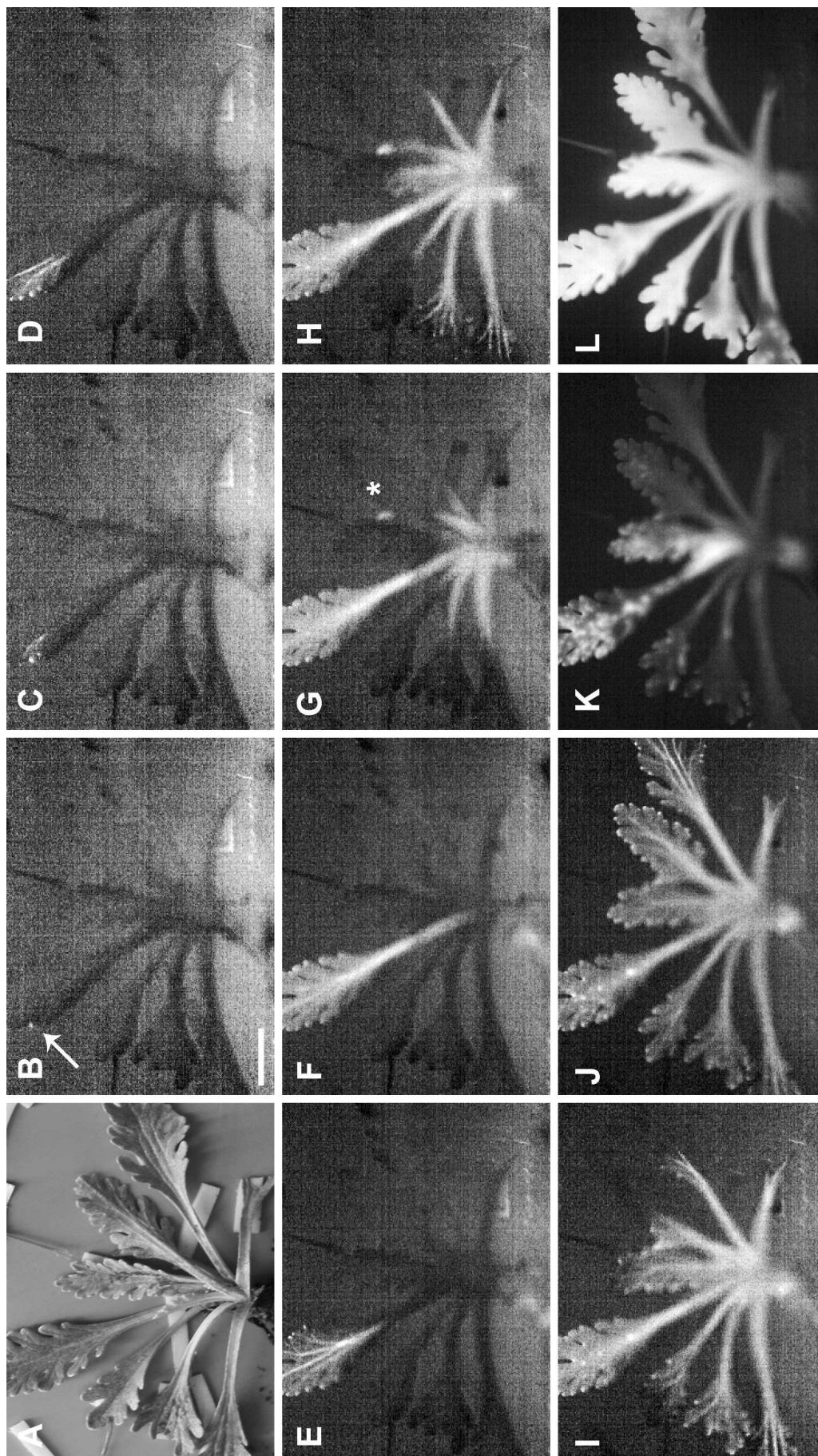
FIGURE 1. Sequence of IDTA images shows the freezing pattern in a (A) whole plant of *S. incanus*. Initial ice nucleation occurred in a leaf blade at an outermost tip of a leaf lob (B, indicated by the arrow). Then ice spread in the vascular tissue of the leaf towards the center of the shoot within 2 s (C–F) and throughout the whole plant within 5.2 s (G–J), visualizing the reticulate venation pattern. In this phase, a second nucleation event could be detected in another leaf (G, indicated by an asterisk). From the xylem, ice propagated into the mesophyll resulting in a brindled freezing pattern on the leaves (K), which is diminished within 30 s (L). Time scale: (B) 0 s, (C) 0.2 s, (D) 0.4 s, (E) 0.8 s, (F) 2 s, (G) 3.6 s, (H) 4 s, (I) 4.4 s, (J) 5.2 s, (K) 10 s, and (L) 30s (length of the bar is 1 cm). Videos showing the freezing of *S. incanus* and the other investigated species described in this article, are available on the web <http://www.uibk.ac.at/botany/stressphysiology>, menu point "Ice propagation."
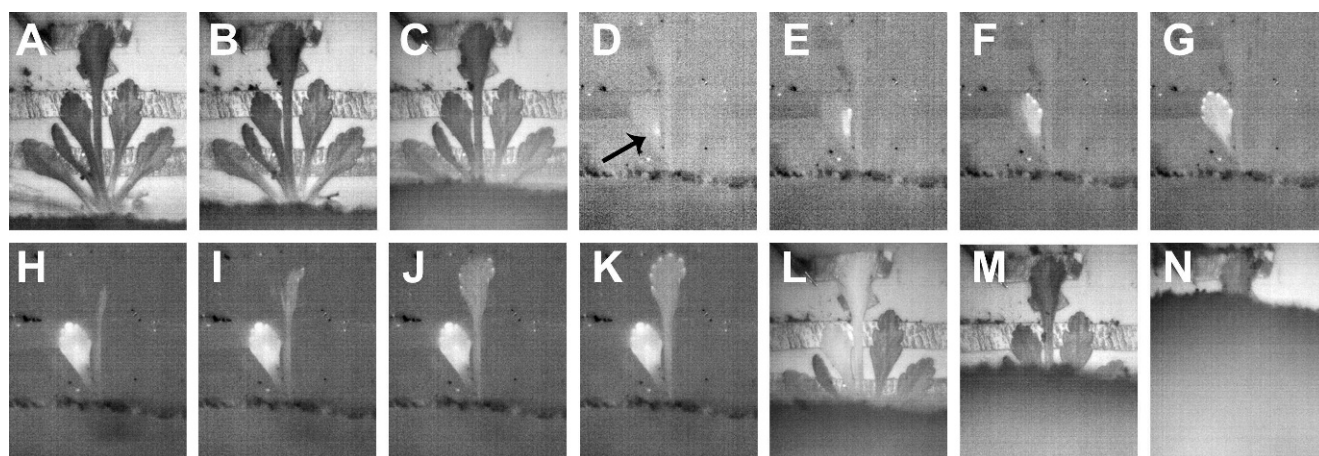
J. HACKER AND G. NEUNER / 663

FIGURE 2. Sequence of infrared images (A–C, L–N) and IDTA images respectively (D–K) showing the freezing of a whole plant of *S. incanus* investigated under radiative freezing conditions. Intrinsic ice nucleation occurred at $-3.5°C$ in the leaf lamina (D, indicated by an arrow) which caused freezing of this (D–G) and a second leaf (H–K). Although the plant was totally covered by snow at the end of the measurement, freezing in the remaining leaves were neither initiated by intrinsic nor by extrinsic nucleation at a leaf temperature of $-5°C$. Time scale for infrared images (A–C, L–N, after the onset of snow fall): (B) 10 min, (C) 20 min, (D) 30 min (L) 35 min, (M) 50 min, and (N) 65 min. Time scale for IDTA images (D–K, 32 min after the onset of snow fall, after the beginning of vascular ice propagation): (E) 0.5 s, (F) 1 s, (G) 1.5 s, (H) 47 s, (I) 47.5 s, (J) 48 s, and (K) 48.5 s.

the leaf surface below the droplet was artificially damaged, ice could easily propagate either from the droplet into the leaf after extrinsic ice nucleation or from the leaf tissue into the droplet after intrinsic ice nucleation. The site of ice nucleation and the temperature of freezing did not affect the general freezing pattern (combination of longitudinal and lateral ice propagation).

Juncus trifidus

The sequence of IDTA images during freezing of a tussock of *J. trifidus* is shown in Figure 5. All shoots of the tussock froze independent from each other, requiring an ice nucleation event in each shoot. In contrast to *P. alpina* the freezing pattern was affected by the degree of supercooling (Fig. 6). While intrinsic ice nucleation at $-6.6°C$ caused freezing of a shoot in a single freezing event affecting all vascular bundles, extrinsic ice nucleation at $-1.7°C$ initiated by INA bacteria resulted in multiple freezing events with ice propagating in both directions. These multiple freezing events either did not show a spatial and temporal relation (Figs. 6E–6G) or seemed to be related, as only 10 s after ice had spread from the base to the tip, ice propagated in the opposite direction (Figs. 6C, 6D).

Silene acaulis

IDTA images during freezing of a whole cushion of *S. acaulis* are shown in Figure 7. Ice nucleation occurred somewhere inside the cushion (but not within the plant tissues themselves) at a temperature of $-0.8°C$. The exact location of this extrinsic ice nucleation event could not be deduced from the IDTA images; it may have occurred in the soil, in the litter, or on the plant surface. After only 10 min, the first intrinsic freezing event within a single cushion shoot was detectable. Freezing of the whole cushion then took 52.5 min, but 30 min after intrinsic ice nucleation, 90% of the cushion was already frozen. Within the freezing process, 30 freezing events, including up to five shoots, could clearly be differentiated. As the stem system was not in focus of the infrared camera, it is difficult to tell whether ice propagated from one shoot to the next or

several intrinsic ice nucleation events occurred. At the end of the freezing treatment all parts of the cushion were frozen.

WHOLE PLANT FREEZING PATTERN

Ice nucleation temperatures varied within a broader temperature range in the investigated graminoids *J. trifidus* and *P. alpina* as compared to the investigated dicotyledonous species *R. ferrugineum* and *S. incanus* (Fig. 8). While ice nucleation did not occur below $-6.3°C$ and $-7.6°C$ in *S. incanus* and *R. ferrugineum*, respectively, supercooling down to $-11.2°C$ and $-13°C$ was observed for *P. alpina* and *J. trifidus*, respectively. The temperature range of whole plant freezing, i.e. the temperature span from the initial ice nucleation event until ice was found in the whole plant was significantly higher in the graminoids. While in *R. ferrugineum* and *S. incanus* one or two nucleation events resulted in freezing of the whole plant, the graminoids required a nucleation event in every leaf, as the single leaves freeze autonomously. The requirement of many nucleation events and the capability for high supercooling enables the graminoids to avoid freezing of the whole plant, when the exposition temperature was above the minimum ice nucleation temperature. Hence, leaves without ice nucleation could survive the freezing treatment (shown for *J. trifidus* in Fig. 5).

RATE OF ICE PROPAGATION

The rate of ice propagation in the veins of leaves increased significantly with decreasing temperature in all investigated species (Fig. 9). When freezing occurred at temperatures of $-2°C$, the rate of ice propagation was low in all species with values between 2 and 3 cm s^{-1}. With increasing supercooling, i.e. lower freezing temperatures, ice propagated much faster, reaching values of up to 24 cm s^{-1} in *J. trifidus*. The linear correlation between the degree of supercooling and the rate of ice propagation was highly significant. The incline of the regression lines was identical for *R. ferrugineum* and *S. incanus*, but was significantly higher in *P. alpina* and even more in *J. trifidus*. This resulted in
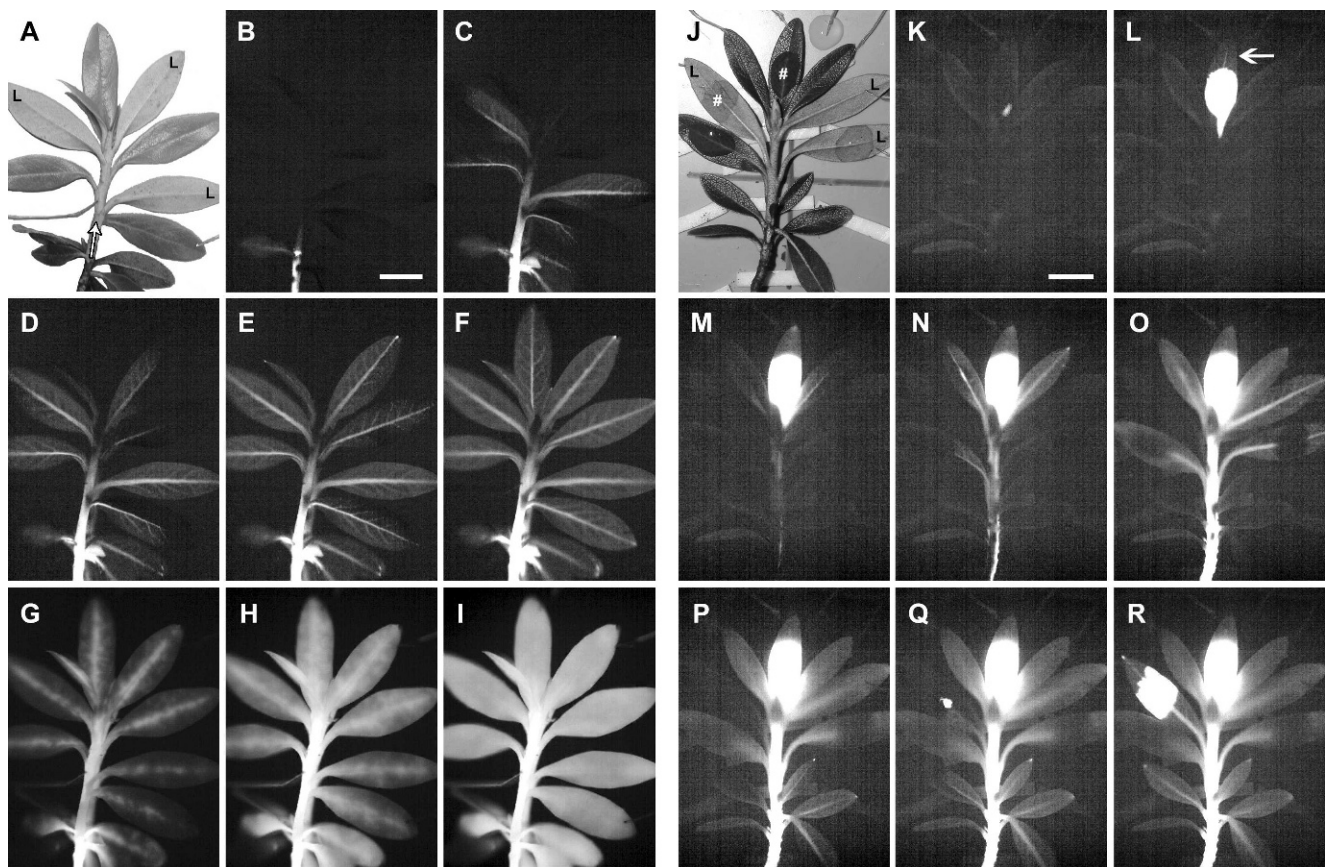
FIGURE 3. Sequences of IDTA images during ice propagation in two plants of *R. ferrugineum* induced by intrinsic ice nucleation (A–I) and extrinsic ice nucleation (J–R). In the first plant (A) intrinsic ice nucleation occurred at −7.3°C in the last year's stem (the border between last year's and this year's sections are indicated by an arrow, leaves are either facing the upper leaf side or the lower leaf side, the latter marked with the letter "L"). Subsequently, ice propagated into the stem and throughout the whole shoot showing the leaf venation pattern. (B–F). After vascular freezing, the onset of mesophyll freezing resulted in a brindled freezing pattern (G and H) which diminished after 1 minute (I). In the second plant (J), water droplets were applied on four leaves either at the upper or the lower leaf side (the latter indicated by the letter "L"), either on an intact or a damaged leaf surface (the latter indicated by a hash). Ice nucleation occurred at −5.3°C in a water droplet, which was located on a leaf with damaged surface (K). Soon after ice came in contact with inner plant tissues, vascular freezing in the same leaf occurred (L, indicated by an arrow), and subsequently ice propagated into the stem and throughout the whole shoot (M–R). Time after intrinsic nucleation (first plant) (B–I): (B) 0.4 s, (C) 1 s, (D) 1.2 s, (E) 1.4 s, (F) 2 s, (G) 10 s, (H) 30 s, and (I) 1 min. Time after extrinsic nucleation (second plant) (K–R): (K) 0.2 s, (L) 0.6 s, (M) 3.4 s, (N) 4.4 s, (O) 6.8 s, (P) 11.8 s, (Q) 12.4 s, and (R) 13.1 s. Length of the bars in B and K is 1 cm.

higher rates of ice propagation in the graminoids at similar freezing temperatures.

Discussion

ICE PROPAGATION AND FREEZING PATTERNS

The determination of ice propagation and freezing patterns at the whole organism level using IDTA revealed substantial differences among the investigated species. In plants with plane leaf blades such as *P. alpina*, *R. ferrugineum*, and *S. incanus* the leaf venation pattern could clearly be visualized during vascular freezing, which was also shown for woody species in Hacker and Neuner (2007). In leaves of *J. trifidus* and *S. incanus,* this was not possible due to the small leaf size (1 mm). Ice propagation patterns in the two investigated graminoids *J. trifidus* and *P. alpina* reflected the influence of the vascular structure on the freezing process, at the leaf level and the whole organism level as well. In *P. alpina* single tracheids laterally interconnect the longitudinal bundles in a ladder-like manner; hence, vascular freezing consists of a longitudinal and a lateral component. Lateral ice propagation cannot be visualized by IDTA, as the distance between longitudinal veins is only 92 µm

and thus below the spatial resolution of the infrared camera; additionally, the released heat resulting from freezing of single tracheids is very small. In contrast, the rush *J. trifidus* lacks these vascular interconnections and the longitudinal bundles are isolated from each other. At high nucleation temperatures induced by application of a bacterial INA suspension, freezing of bundles seemed to be facilitated by ice propagation within non-vascular tissue or an upturn of ice propagation at the leaf tip.

Leaves and shoots of graminoid tussocks froze independent from each other as ice could not propagate from one leaf to another via the stem. This has already been reported for other graminoid species (Pearce and Fuller, 2001; Stier et al., 2003). The IDTA records reveal ice propagating throughout the vascular bundles of the leaf blade and leaf sheath into the stem. The polystele of monocotyledonous stems prevents ice propagation via the vascular system into other leaves. Leaf vascular bundles do not end blindly in the stem, but are usually linked with strands of older leaves via nodal plexus branches (Esau, 1965; Hitch and Sharman, 1971; Shane et al., 2000). Although this linkage allows the conduit of water, ice propagation seems to be blocked.

In *S. acaulis*, initial freezing was always extrinsic and occurred inside the cushion (litter, soil). Only after a distinct
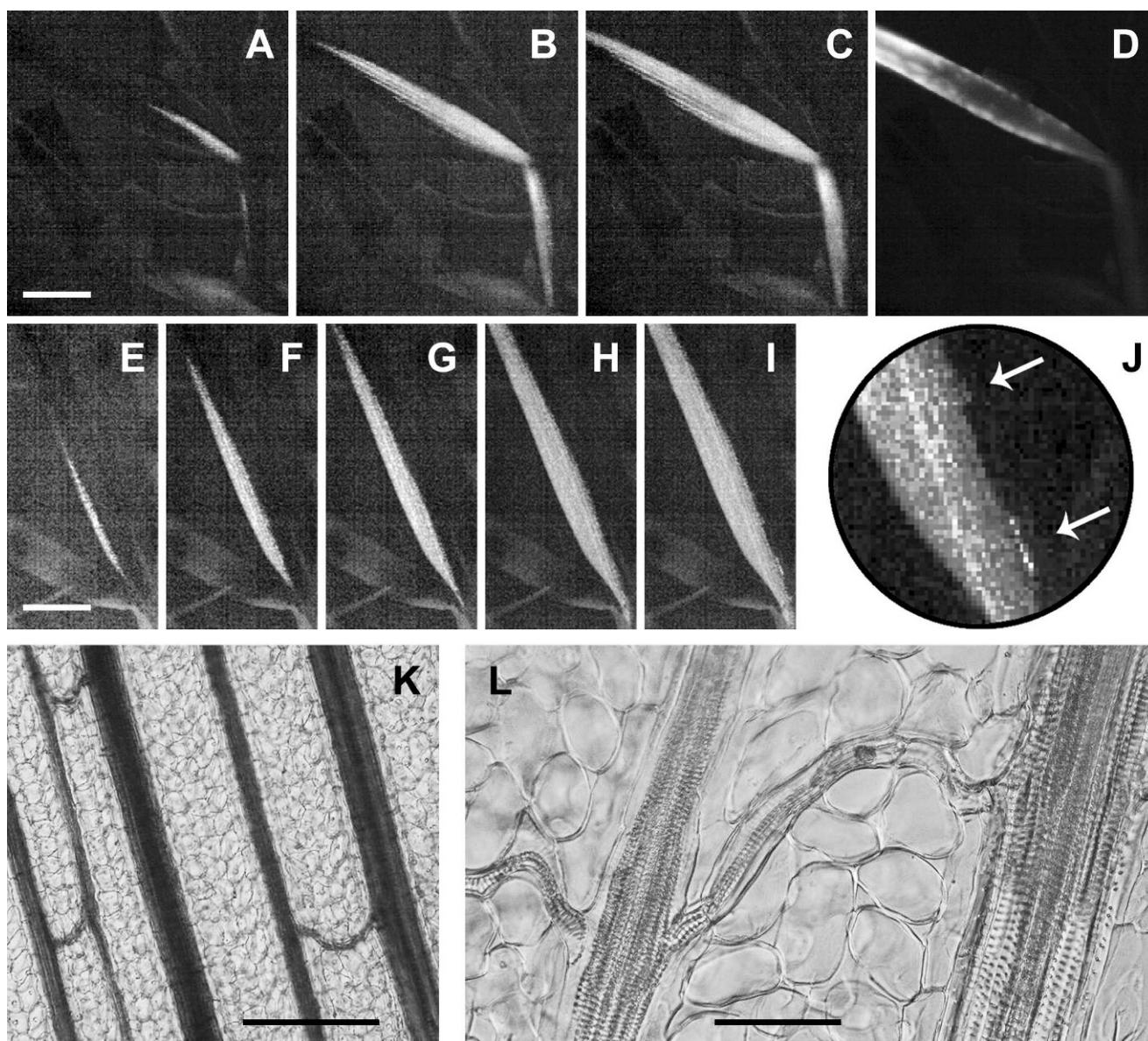
J. Hacker and G. Neuner / 665

FIGURE 4. Sequences of IDTA images of ice propagation in leaves of two shoots of the alpine grass *P. alpina* show the parallel venation patterns typical of monocotyledonous plants and the combination of longitudinal and lateral vascular ice propagation. In the first leaf (A–D) ice nucleation occurred at the boundary between the leaf sheath and the leaf blade (A). Ice propagated within the vascular tissue towards the leaf tip and sheath base (A–C), freezing of the mesophyll resulted in a brindled freezing pattern on the lamina (D). In the second shoot (E–J) the occurrence of lateral ice propagation between neighboring parallel main veins interconnected by lateral single tracheids (K and L) is shown. Lateral ice propagation cannot be visualized by IDTA as the distance between the parallel main veins is too small (92 ± 10 μm) to be resolved by the infrared camera. However, lateral ice propagation can be detected indirectly by continued ice propagation in a neighboring vein (I and J; sites of lateral ice propagation are indicated by arrows in the detail figure). Time after nucleation (A–D): (A) 0.2 s, (B) 0.6 s, (C) 0.8 s, and (D) 5.8 s; (E–J): (E) 160 ms, (F) 320 ms, (G) 400 ms, (H) 560 ms, and (I and J) 640 ms (length of the bars: A and E: 1 cm, K: 200 μm, L: 50 μm).

delay, freezing of single shoots was detected; the freezing pattern of the whole cushion consisted of many separate freezing events of single shoots. Whether these freezing events were induced by independent intrinsic ice nucleation or by delayed ice propagation between shoots could not be determined by IDTA due to the highly complex aboveground plant structure of the cushion. Leaf and branch junctions are known as potential water flow constrictions and segmentation points in the hydraulic architecture (Schulte and Brooks, 2003). The sectoriality of the vascular system describes the degree of hydraulic coupling between plant parts, which may range from full coupling to limited interconnectedness (Brooks et al., 2003; Schulte and Brooks, 2003; Orians et al, 2005; Ellmore et al, 2006; Zanne et al., 2006). Hydraulic

sectoriality may explain the freezing pattern in *S. acaulis* with its highly branched shoot and *S. incanus* with leaves emerging from a compressed stem.

ECOLOGICAL CONSIDERATIONS

The number of ice nucleation events necessary for whole plant freezing and the temperature range wherein whole plant freezing occurred increased from woody and herbaceous plants to cushions and increased significantly further to the graminoids. In herbaceous and woody plants, one ice nucleation event caused immediate freezing of the whole plant, as there were no ice barriers. No specific effect on frost survival may be derived from
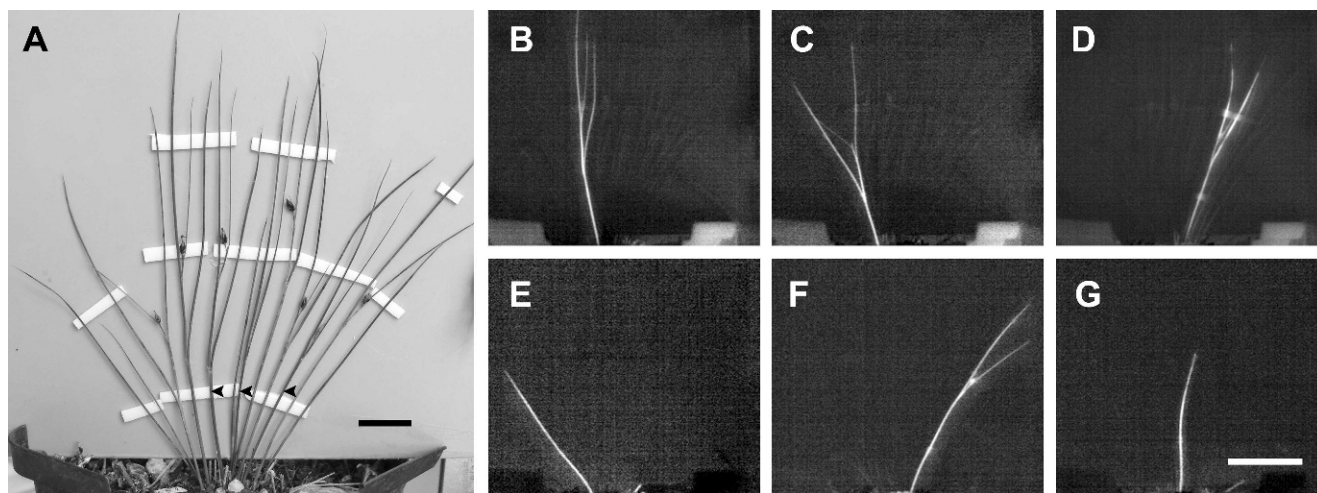
FIGURE 5. The sequence of IDTA images shows freezing of the single shoots of a tussock of *J. trifidus* (A) independently of each other within 87 min after the first freezing event. Intrinsic ice nucleation occurred either between −6.7 and −12°C or not at all. Without intrinsic ice nucleation shoots remained undamaged (black arrowheads in A indicate undamaged shoots). Time after the first ice nucleation event in B: (C) 34 min, (D) 39 min, (E) 54 min, (F) 63 min, and (G) 87 min (Length of the bars: A: 1 cm, G: 3 cm).

this ice propagation pattern and at least for some alpine plants it is known that they depend more on repair and replacement of vegetative tissue lost after frost damage than on high summer frost resistance (Körner, 1999; Taschler and Neuner, 2004). The rate of ice propagation and mesophyll dehydration is distinctly slowed down at higher ice nucleation temperatures (Hacker and Neuner, 2007) and might even result in less frost damage as extended supercooling may cause more severe frost damage (Sakai and Larcher, 1987).

For cushion plants during summer night frosts, thermal buffering by freezing of water externally sucked up by litter and debris within the compact cushion could be an important frost survival mechanism (Sakai and Larcher, 1987). The heat of crystallization released during freezing of this external water inside compact cushion plants such as *S. acaulis* can keep the plant temperature at moderate freezing temperatures ($> -2°C$) for several hours until all of the adhering water is frozen. Hence, the living plant parts that freeze *in situ* at mean temperatures of −3.5°C (Taschler and Neuner, 2004) may be protected from lethal freezing temperatures throughout a whole summer night frost (Sakai and Larcher, 1987). In graminoids, each leaf needs an autonomous ice nucleation event. This freezing pattern of the graminoids combined with a high supercooling ability may explain why graminoids had the highest summer frost hardiness among alpine plant species (Taschler and Neuner, 2004). Air temperature minima indicate that the investigated plants may suffer frost damage at their natural growing sites (see Fig. 4 *in* Taschler and Neuner, 2004). Hence, the freezing pattern observed in graminoids may be advantageous for survival at alpine sites.
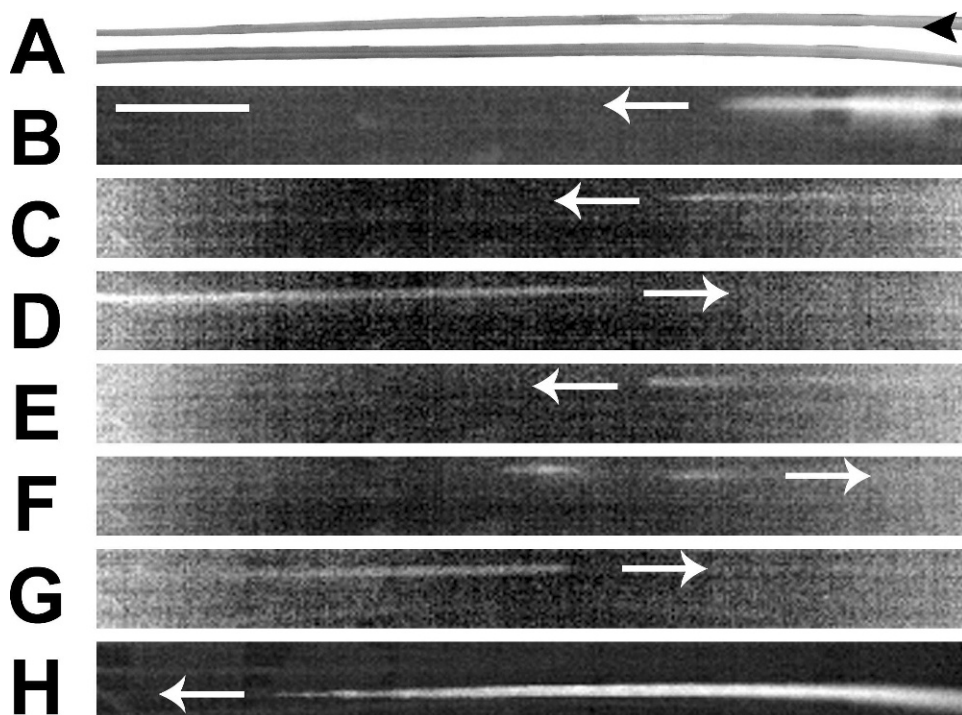

FIGURE 6. The freezing pattern of two shoots of *J. trifidus* (A) changed according to their freezing temperature. In one leaf ice nucleation at −1.7°C was initiated by INA bacteria (applied at the leaf base, indicated by a black arrowhead) which caused multiple freezing events within 17.3 min shown in a sequence of IDTA images (B–G, direction of ice propagation indicated by the arrows). In a second shoot intrinsic ice nucleation at −6.6°C caused freezing of the whole shoot during a single freezing event. Time after the first freezing event in B: (C) 10.7 min, (D) 10.9 min, (E) 14 min, (F) 14.2 min, (G) 17.3 min, and (H) 84.7 min (Length of the bar is 1 cm).
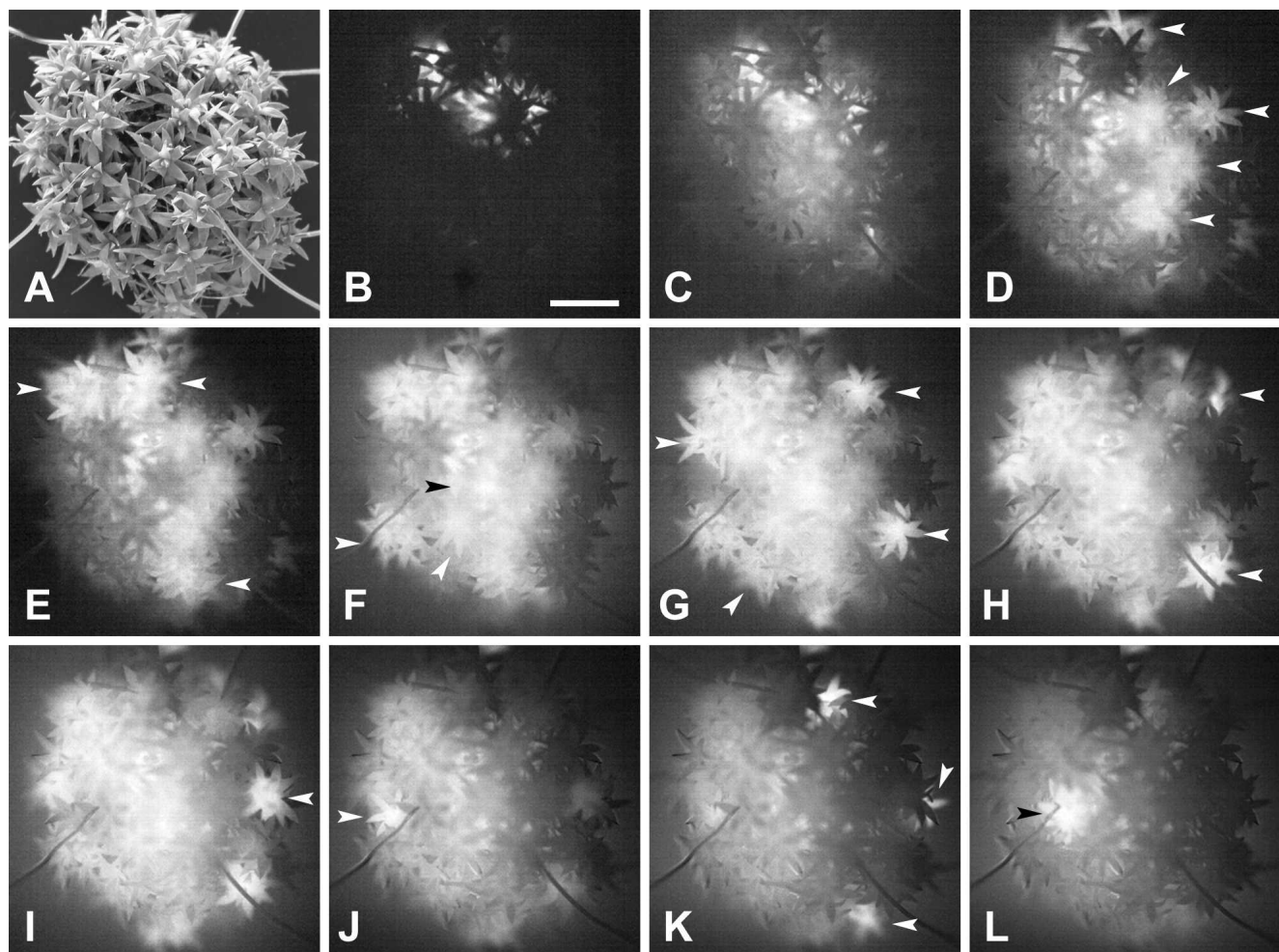
J. HACKER AND G. NEUNER / 667

FIGURE 7. Freezing in the alpine cushion plant *S. acaulis* (A) is shown by a sequence of IDTA images (B–L). Initial freezing first occurred somewhere inside the cushion (B); the exact location cannot be deduced from the IDTA image. After only 10 min (D) intrinsic freezing of single shoots of the cushion was detectable (white arrowheads indicate freezing of single shoots). Freezing of the whole cushion took 27 min. Time after initial freezing in B: (C) 5 min, (D) 10 min, (E) 12.5 min, (F) 15 min, (G) 17 min, (H) 20 min, (I) 21 min, (J) 30 min, (K) 33.5 min, and (L) 37 min (length of the bar in B is 1 cm).

INTRINSIC VERSUS EXTRINSIC NUCLEATION

In natural habitats, the efficiency of supercooling as a frost survival mechanism will also depend on the question of formation of surface ice. Bacterial ice nucleators are commonly present on plant surfaces (Hirano and Upper, 2000). They are only active in aqueous solutions and thus surface moisture is a prerequisite for extrinsic ice nucleation (Wisniewski et al., 2002b). In a natural setting during radiative cooling plants can be exposed to dew formation on the plant surface. This dew provides the surface moisture required for the activation of INA bacteria that are likely to cause external ice nucleation at higher temperatures. Hence supercooling as observed in our laboratory experiments will only be possible at natural growing sites if ice growth from extrinsic nucleation sites into the plant is impaired. Frozen droplets of water or bacterial suspension applied on the leaf surface of *P. alpina*, *S. incanus*, and *R. ferrugineum* could not induce intrinsic ice nucleation as long as the leaf epidermis was undamaged. In contrast, frozen droplets applied on damaged leaf surfaces induced freezing of the plant in all investigated species. The freezing patterns were independent of the ice nucleation source (either water or INA bacteria). When INA bacteria at $-2.5°C$ induced extrinsic nucleation, the freezing pattern was not altered, but the rates of ice propagation were lower. This corresponds to earlier observations that external ice does not necessarily induce intrinsic

freezing, as the external ice first has to propagate into the plant (Wisniewski et al., 2002a). Ice propagation can be through stomata in some species (*Phaseolus vulgaris, Prunus domestica, Malus domestica*: Wisniewski et al., 1997; Wisniewski and Fuller, 1999), but only via a damaged cuticle or other lesions in *Rhododendron* sp. (Wisniewski et al., 1997), *Lolium perenne*, and *Poa supina* (Stier et al., 2003). Leaf wettability is also an important factor in protecting the leaf from extrinsic ice nucleation. Applying a hydrophobic particle film can prevent extrinsic ice nucleation, which prevents ice growth from the surface into the plant and hence frost damage (Wisniewski et al., 2002b; Fuller et al., 2003). Preliminary results indicate that leaf wettability is reduced in most alpine plants (Aryal and Neuner, unpublished data).

RATE OF ICE PROPAGATION

Our results corroborate earlier findings (Hacker and Neuner, 2007; Kitaura, 1967; Pearce and Fuller, 2001) that a major determinant of the rate of ice propagation is the ice nucleation temperature, i.e. supercooling will markedly speed up ice propagation in plants. The rate of ice propagation increased significantly with decreasing freezing temperature in the investigated plant species (*J. trifidus*, *P. alpina*, *R. ferrugineum*, and *S. incanus*). Hacker and Neuner (2007) found the same relationship for
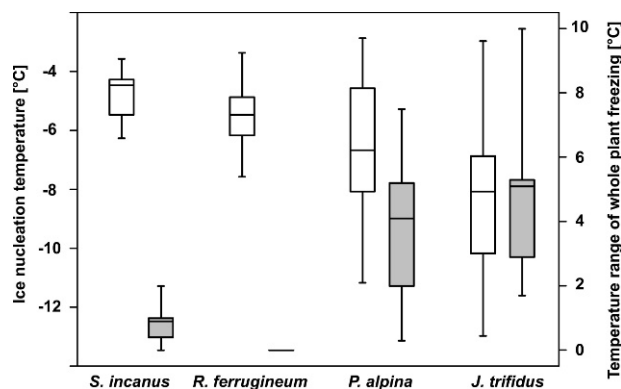
FIGURE 8. Ice nucleation temperatures (boxplots with white filling) were significantly lower in *J. trifidus* and were widely scattered between −3 and −13°C. In the second graminoid *P. alpina*, ice nucleation temperatures varied also in a broad temperature range. This was in contrast to the two dicotyledonous species *R. ferrugineum* and *S. incanus*. The temperature range of freezing of a whole shoot (boxplots with gray filling) differed significantly between the two graminoids on the one hand, and *R. ferrugineum* and *S. incanus* on the other hand. Whole herbaceous and woody plants freeze within a short period of time usually after one initial ice nucleation event, while freezing of graminoids takes significantly longer, as multiple ice nucleation events are necessary for the freezing of the whole plant (boxplots show median, 25th percentile, 75th percentile, maximum, and minimum).
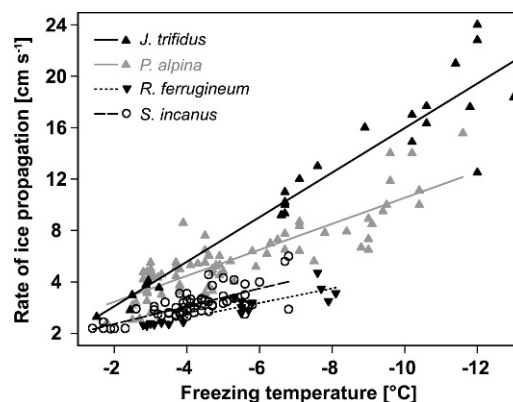

FIGURE 9. The rate of longitudinal ice propagation in main veins of leaves is displayed as a function of freezing temperature (the straight line represents regression lines). The rate of ice propagation is not species specific but increases with decreasing freezing temperature for all investigated species. Correlation analysis reveals a highly significant linear relationship between the rate of ice propagation and freezing temperature (correlation coefficients r^2 after Pearson: *J. trifidus* (0.89), *P. alpina* (0.74), *R. ferrugineum* (0.80), and *S. incanus* (0.52); $P < 0.01$).

woody species (*B. sempervirens*, *C. camphora*, *F. sylvatica*, *Q. robur*, and *T. baccata*). Ice growth in an aqueous solution depends mainly on thermal phenomena occurring at the solid-liquid interface (Ayel et al., 2006; Liu et al., 2004; Shibkov et al., 2004). Three factors limit the ice growth rate: (1) the diffusion of heat and solute away from the solid-liquid interface, (2) the tension between the ice and the solution, and (3) the kinetics of attachment of water molecules to the ice surface (Liu et al., 2004). The latter can be neglected, as the cooling rates in biological systems are not high enough.

The investigated graminoids *J. trifidus* and *P. alpina* showed significantly higher rates of ice propagation compared with other herbaceous and woody species at similar temperatures. A peculiarity of monocotyledonous leaves is the existence of protoxylem besides metaxylem vessels in some of the larger longitudinal bundles (Dannenhoffer and Evert, 1994; Martre et al., 2000). Protoxylem vessels ensure vascular continuity in the growth zone of grass leaves. During further growth, the protoxylem vessels mainly collapse and are replaced by a lacunae. This protoxylem lacunae is water filled and functions as a water-conducting conduit continuous throughout the leaf (Dong et al., 1997; Martre et al., 2000; Canny, 2001).

In intact vessels, moving water has to pass the pit membranes at the end walls. The small pore sizes (estimated average pore diameter in dicotyledonous trees: 5–20 nm (Choat et al., 2003) generate a significant hydraulic resistance (Choat et al., 2006) which may account for up to 87% total vascular resistance (Schulte and Gibson, 1988; Sperry et al., 2005; Choat et al., 2006). Pit membranes may also represent an efficient barrier for ice propagation that is known to be suppressed in capillaries below 5 nm (Muldrew et al., 2000). In the water filled protoxylem lacunae, fast ice propagation is possibly enabled by the lack of pit membranes. Hence, ice propagation in the two investigated graminoids may occur in the protoxylem lacunae, indicated by the faster ice propagation.

CONCLUSION

IDTA has proven to be an efficient method to investigate freezing on a whole plant level and revealed distinct freezing patterns in the investigated species. The various freezing patterns and ice propagation velocities reflect differences in the hydraulic systems of the plants. Additional investigations of the sectoriality and synchronization with the freezing pattern could further elucidate the pathway of ice propagation. Whole plant freezing patterns can explain the results of summer frost resistance of alpine plants. Graminoids may gain an advantage for frost survival due to enhanced supercooling ability combined with independent freezing of single leaves. Ice at the plant surface acted as an extrinsic ice nucleator only, when the surface was damaged, enabling the contact between ice and inner tissues; an intact epidermal layer prevented freezing of the plant. The freezing patterns themselves were not affected by the source of ice nucleation. Convective cooling has been shown to be a viable method for investigation of freezing patterns, as the freezing patterns were similar under radiative cooling conditions. The main difference between these treatments is dew formation on the plant surface under radiative conditions that will possibly enable extrinsic ice formation. Under convective conditions due to a dry surface plant freezing is always initiated by intrinsic ice nucleation. When the epidermal layer is intact, extrinsic ice will have no influence, but in case of injuries, it will be the starting point of freezing. Although the freezing pattern did not change, freezing at higher temperatures will cause freezing and withdrawal of water from cells at more moderate rates, which can be advantageous for plant survival.

References Cited

Ayel, V., Lottin, O., Faucheux, M., Sallier, D., and Peerhossaini, H., 2006: Crystallisation of undercooled aqueous solutions: experimental study of free dendritic growth in

cylindrical geometry. *International Journal of Heat and Mass Transfer*, 49: 1876–1884.

Ball, M. C., Wolfe, J., Canny, M., Hofmann, M., Nicotra, A. B., and Hughes, D., 2002: Space and time dependence of temperature and freezing in evergreen leaves. *Functional Plant Biology*, 29: 1259–1272.

Brooks, J. R., Schulte, P. J., Bond, B. J., Coulombe, R., Domec, J. C., Hinckley, T. M., McDowell, N., and Phillips, N., 2003: Does foliage on the same branch compete for the same water? Experiments on Douglas-fir trees. *Trees—Structure and Function*, 17: 101–108.

Burke, M., Gusta, L., Quamme, H., Weiser, C., and Li, P., 1976: Freezing and injury in plants. *Annual Review of Plant Physiology and Plant Molecular Biology*, 27: 507–528.

Canny, M. J., 2001: Embolisms and refilling in the maize leaf lamina, and the role of the protoxylem lacuna. *American Journal of Botany*, 88: 47–51.

Carter, J., Brennan, R., and Wisniewski, M., 2001: Patterns of ice formation and movement in blackcurrant. *Hortscience*, 36: 855–859.

Choat, B., Ball, M., Luly, J., and Holtum, J., 2003: Pit membrane porosity and water stress-induced cavitation in four co-existing dry rainforest tree species. *Plant Physiology*, 131: 41–48.

Choat, B., Brodie, T. W., Cobb, A. R., Zwieniecki, M. A., and Holbrook, N. M., 2006: Direct measurements of intervessel pit membrane hydraulic resistance in two angiosperm tree species. *American Journal of Botany*, 93: 993–1000.

Dannenhoffer, J. M., and Evert, R. F., 1994: Development of the vascular system in the leaf of barley (*Hordeum vulgare* L.). *International Journal of Plant Sciences*, 155: 143–157.

Dong, Z., McCully, M. E., and Canny, M. J., 1997: Does *Acetobacter diazotrophicus* live and move in the xylem of sugarcane stems? Anatomical and physiological data. *Annals of Botany*, 80: 147–158.

Ellmore, G. S., Zanne, A. E., and Orians, C. M., 2006: Comparative sectoriality in temperate hardwoods: hydraulics and xylem anatomy. *Botanical Journal of the Linnean Society*, 150: 61–71.

Esau, K., 1965: *Plant anatomy*. New York: John Wiley & Sons, 767 pp.

Fuller, M., Hamed, F., Wisniewski, M., and Glenn, D. M., 2003: Protection of plants from frost using hydrophobic particle film and acrylic polymer. *Annals of Applied Biology*, 143: 93–97.

Hacker, J., and Neuner, G., 2007: Ice propagation in plants visualized at the tissue level by infrared differential thermal analysis (IDTA). *Tree Physiology*, 27: 1661–1670.

Hirano, S. S., and Upper, C. D., 2000: Bacteria in the leaf ecosystem with emphasis on *Pseudomonas syringae*—A pathogen, ice nucleus, and epiphyte. *Microbiology and Molecular Biology Reviews*, 64: 624–653.

Hitch, P. A., and Sharman, B. C., 1971: Vascular pattern of festucoid grass axes, with particular reference to nodal plexi. *Botanical Gazette*, 132: 38–56.

Jordan, D., and Smith, W., 1994: Energy balance analysis of nighttime leaf temperatures and frost formation in a subalpine environment. *Agricultural and Forest Meteorology*, 71: 359–372.

Kitaura, K., 1967: Supercooling and ice formation in mulberry trees. *In* Asahina, E. (ed.), *Cellular injury and resistance in freezing organisms. International conference on low temperature science. Vol. II: Conference on cryobiology*. Hokkaido University: The Institute of Low Temperature Science, 143–156.

Körner, C., 1999: *Alpine plant life. Functional plant ecology of high mountains ecosystems*. Berlin: Springer, 338 pp.

Lindow, S. E., and Brandl, M. T., 2003: Microbiology of the phyllosphere. *Applied and Environmental Microbiology*, 69: 1875–1883.

Liu, Z. H., Muldrew, K., Wan, R. G., and Elliott, J. A. W., 2004: Retardation of ice growth in glass capillaries: measurement of the critical capillary radius. *Physical Review E*, 69: 021611.

Maki, L. R., Galyan, E. L., Changchi, M., and Caldwell, D. R., 1974: Ice nucleation induced by *Pseudomonas syringae*. *Applied Microbiology*, 28: 456–459.

Martre, P., Durand, J. L., and Cochard, H., 2000: Changes in axial hydraulic conductivity along elongating leaf blades in relation to xylem maturation in tall fescue. *New Phytologist*, 146: 235–247.

Muldrew, K., Novak, K., Yang, H., Zernicke, R., Schachar, N. S., and McGann, L. E., 2000: Cryobiology of articular cartilage: ice morphology and recovery of chondrocytes. *Cryobiology*, 40: 102–109.

Orians, C. M., Smith, S. D. P., and Sack, L., 2005: How are leaves plumbed inside a branch? Differences in leaf-to-leaf hydraulic sectoriality among six temperate tree species. *Journal of Experimental Botany*, 56: 2267–2273.

Pearce, R. S., and Fuller, M. P., 2001: Freezing of barley studied by infrared video thermography. *Plant Physiology*, 125: 227–240.

Sakai, A., and Larcher, W., 1987: *Frost survival of plants. Responses and adaptation to freezing stress*. Berlin: Springer Verlag, 321 pp.

Schulte, P., and Gibson, A., 1988: Hydraulic conductance and tracheid anatomy in 6 species of extant seed plants. *Canadian Journal of Botany*, 66: 1073–1079.

Schulte, P. J., and Brooks, J. R., 2003: Branch junctions and the flow of water through xylem in Douglas-fir and ponderosa pine stems. *Journal of Experimental Botany*, 54: 1597–1605.

Sekozawa, Y., Sugaya, S., and Gemma, H., 2004: Observations of ice nucleation and propagation in flowers of Japanese pear (*Pyrus pyrifolia* Nakai) using infrared video thermography. *Journal of the Japanese Society for Horticultural Science*, 73: 1–6.

Shane, M. W., McCully, M. E., and Canny, M. J., 2000: The vascular system of maize stems revisited: implications for water transport and xylem safety. *Annals of Botany*, 86: 245–258.

Shibkov, A. A., Zheltov, M. A., Korolev, A. A., Kazakov, A. A., and Leonov, A. A., 2004: Effect of surface kinetics on the dendritic growth of ice in supercooled water. *Crystallography Reports*, 49: 1056–1063.

Sperry, J. S., Hacke, U. G., and Wheeler, J. K., 2005: Comparative analysis of end wall resistivity in xylem conduits. *Plant Cell and Environment*, 28: 456–465.

Stier, J. C., Filiault, D. L., Wisniewski, M., and Palta, J. P., 2003: Visualization of freezing progression in turfgrasses using infrared video thermography. *Crop Science*, 43: 415–420.

Taschler, D., and Neuner, G., 2004: Summer frost resistance and freezing patterns measured *in situ* in leaves of major alpine plant growth forms in relation to their upper distribution boundary. *Plant Cell and Environment*, 27: 737–746.

Wisniewski, M., and Fuller, M., 1999: Ice nucleation and deep supercooling in plants: new insights using infrared thermography. *In* Margesin, R., and Schinner, F. (eds.), *Cold adapted organisms. Ecology, physiology, enzymology and molecular biology*. Berlin: Springer Verlag, 105–118.

Wisniewski, M., Lindow, S. E., and Ashworth, E. N., 1997: Observations of ice nucleation and propagation in plants using infrared video thermography. *Plant Physiology*, 113: 327–334.

Wisniewski, M., Fuller, M., Glenn, D., Gusta, L., Duman, J., and Griffith, M., 2002a: Extrinsic ice nucleation in plants: what are the factors involved and can they be manipulated? *In* Li, P. H., and Palva, E. T. (eds.), *Plant cold hardiness. Gene regulation and genetic engineering*. New York: Kluwer Academic Publishers, 223–236.

Wisniewski, M., Glenn, D. M., and Fuller, M. P., 2002b: Use of a hydrophobic particle film as a barrier to extrinsic ice nucleation in tomato plants. *Journal of the American Society for Horticultural Science*, 127: 358–364.

Workmaster, B., Palta, J., and Wisniewski, M., 1999: Ice nucleation and propagation in cranberry uprights and fruit using infrared video thermography. *Journal of the American Society for Horticultural Science*, 124: 619–625.

Zanne, A. E., Sweeney, K., Sharma, M., and Orians, C. M., 2006: Patterns and consequences of differential vascular sectoriality in 18 temperate tree and shrub species. *Functional Ecology*, 20: 200–206.